MULTIVARIATE OPTIMIZATION OF PYROLYSIS PROCESS PARAMETERS FOR BIOCHAR PRODUCTION DERIVED FROM DEMINERALIZED POULTRY LITTER USING RESPONSE SURFACE METHODOLOGY

Kevin Nyoni, Leungo Kelebopile

Department of Mechanical, Energy & Industrial Engineering, Botswana International University of Science and Technology, Botswana, kevin.nyoni@studentmail.biust.ac.bw

Poultry litter is an abundant agricultural waste that poses a health risk when improperly disposed. To mitigate this problem, poultry litter can be used as fuel in combustion. The objective is to develop models that can optimize pyrolysis parameters for improved biochar quality and yield. Prior, the poultry litter is demineralized to reduce inorganic elements. RSM–CCD method developed models and optimized temperature, particle size, and reaction time to determine the outputs (biochar yield, higher heating value, H/C ratio, and energy yield). The developed models were significant with a p–value < 0.05. Maximum biochar yield (59.49%) was obtained at optimum pyrolysis parameters of 300 °C, 2.47mm, and 15 min. Maximum higher heating value (22.2MJKg^{-1}) and energy yield (70.00%) were obtained at 300 °C, 4.04mm, and 15 min. Low H/C ratio was 0.03 at 550 °C, 1.17mm, and 15 min. ANOVA analysis verified the validity and degree of fitness of the developed models. Low standard deviation (< 7.00), small coefficient of variation (< 14.00%), high R^2 (> 0.80), low difference of Adjusted R^2 and Predicted R^2 (< 0.20) and high adequate precision (> 4.00) verified the model's adequacy for good precision. Models' desirability function was satisfactory (> 4) with a 5.00% deviation from experimental values.

Key words: Biochar, Central composite design, Demineralized poultry litter, Pyrolysis, Response surface methodology.

Received 31. 07. 2023, Accepted 14. 09. 2023

1. Introduction

The world's energy consumption has been substantially increasing at a 5.00% per annum growth rate in the past decade due to global population growth (1.10% per annum) and industrialization [1,2]. Such an increase in growth has resulted in depending heavily on fossil fuels for energy production due to their availability in abundance. However, fossil fuels are not renewable and when combusted they contribute to the emissions of greenhouse gases (CO_2, NO_x, and SO_x) which results in an increase of the earth's surface temperature [3]. An alternative fuel source is relevant to substitute the application of fossil fuels, and biomass energy has that potential. Biomass is a heterogeneous organic matter derived from different sources such as agricultural waste, human waste, and forest that can be used for energy applications as it is renewable, low cost and has an almost net zero CO_2 emission [4]. Biomass accounts for 14.00% of the global energy consumption while ranked fourth as the most utilized energy source [5].

Poultry litter is a potential biomass waste that can be utilized to supplement fossil fuels due to its abundant availability, with its poultry production industry occupying 47.00% of the global agriculture sector [6]. Such resource (poultry litter) must be disposed of properly to avoid water contamination through leaching of its inorganic elements and to reduce flies as they are vectors for bacteria that pose a risk to human and animal health [7]. To counter these adverse effects, poultry litter waste can be utilized as a raw material for energy production [8].

Poultry litter resembles uneven particle sizes, high ash, high moisture, high inorganic elements, and low energy content [9]. When combusted, the poultry litter produces a low flame temperature that reduces the thermal combustion performance. This promotes the production of particulate and CO_X emissions, which tend to pollute the environment and corrode or agglomerate the reactors [10]. To reduce the mentioned combustion effects caused by poultry litter, the feedstock is pretreated by demineralizing and thermochemical converting to biochar, bio-oil, or biogas [10].

Demineralization reduces the composition of inorganic elements in poultry litter, thus improving the feedstock quality. The demineralization is categorized as mechanical size fractioning or solvent treatment. Mechanical size fractioning separates the inorganic elements by sieving the poultry litter into different particle-size segments [11]. Solvent treatment can be either acid or water leach treatment. Acid leach treatment reduces the inorganic elements by using acid–aqueous solvents (AcOH, H_2SO_4) to dissolve elements, whereas the water solvent utilizes tap water or deionized water to dissolve the elements [12]. Compared to water treatment, the acid treatment effectively reduces the inorganic elements; however, its application can change the poultry litter's physicochemical structure [13]. Water treatment is easy to use and inexpensive, and it only dissolves the soluble inorganic elements without affecting the biomass composition [13].

Pyrolysis is commonly used to thermochemical convert poultry litter into biofuels (biochar, bio–oil, or biogas). The biofuels produced have better physicochemical

properties and high energy content than untreated poultry litter. The quantity of biochar, bio–oil, or biogas produced after the pyrolysis reaction depends on the reactor temperature, residence time, heating rate, feedstock particle size, pressure, and reactor design [14]. To favor more production of biochar over bio–oil and biogas, the pyrolysis reaction parameters should have a long residence time (>1hr), low reaction temperature (300–500 °C), and low heating rate (5–20 °Cmin^{-1}) [15]. Song and Guo [16] noted a high biochar yield of 45.71–60.10% at temperature range of 300–500 °C and particle size < 4.00mm when poultry litter was pyrolyzed. For energy application, high quality biochar has a carbon mass fraction and H/C ratio of ≥ 50.00% and < 0.70 [17].

In this study, application of quality biochar derived from pyrolyzed demineralized poultry litter is desired as the fuel will combust efficiently with little particulate matter containing inorganic elements being emitted while producing a high energy yield compared to its parent biomass. According to literature review, most studies have used one-factor-at-a-time method (OFAT) to explore and determine the pyrolysis parameters that yield high biochar derived from demineralized poultry litter [15]. The main drawback of OFAT is that it is a time-consuming, money-consuming and cannot quantify the simultaneous interaction relationship between pyrolysis parameters and the response (yield and quality), especially when factoring multiple response outputs [18]. However, the response surface methodology (RSM) can be used to fix these flaws. RSM primarily consists of statistical and mathematical techniques for designing experimental architecture, empirically modelling the process conditions with one or more outputs, analyzing the individual and combined effects of the process conditions, and ultimately determining the best–optimized conditions to obtain the desired or ideal output, all with condensed real experimental trials [19]. RSM has the ability to relate non-linear multivariable data to predict responses with high precision of accuracy. In order to compare the effect of the pyrolysis parameters on multiple output responses, the desirability function normalizes the responses to a range between 0 and 1 [18]. For example, an entirely undesirable reaction has a desirability rating of 0, while an entirely desired response has a value of 1 [20]. As a result, the best-suited parametric condition for optimization is one with a desirable value closer to 1.

The study uses the RSM method to develop multiple models that can optimize the production of biochar from demineralized poultry litter using pyrolysis process. The models developed will predict biochar yield, higher heating value, H/C ratio, and energy yield.

2. Experimental part

2.1. Collection and demineralization of poultry litter

For this study, samples of poultry litter (sunflower husks, wood shavings, and manure) were gathered from Tshipane farm in Palapye, Botswana. The feedstock was dried in an oven (Systronix Scientific, 278, South Africa) for 24hrs at 105 °C and grinded using a ball mill (Pulveisette 6, FRITSCH, Germany) for 15 min. The collected poultry litter was demineralized by washing with deionized water at a biomass-to-solvent ratio of 1:10 (w/v) at 25 °C for 2hrs while being stirred continuously with a magnetic stirrer [21]. The samples were later rinsed with deionized water until a pH (Envtek, ENV49, India) of 7 was reached, dried in an oven at 105 °C for 24hrs, and sealed in a desiccator [12]. After demineralization, the samples were characterized for their physicochemical properties (Proximate, ultimate, and higher heating value). Proximate analysis was carried out using a thermogravimetric analyzer (Leco TGA 701, USA) according to ASTM D7582 MVA standard [22]. Ultimate analysis was carried out using an elemental analyzer (Thermo scientific flash 2000 CHNS/O, USA) measured according to the ASTM D5291–96 standard [23]. An oxygen bomb calorimeter (IKA C6000, USA) measured the higher heating value according to the ASTM D5865–12 [24]. The proximate, ultimate, and higher heating value of the demineralized poultry litter are shown in Table 1.

Table 1 Proximate, ultimate analysis and higher heating value of demineralized poultry litter.

Proximate analysis [weight %, dry basis]	
Moisture content	5.37
Volatile matter	72.10
Ash content	8.16
Fixed carbon	19.74
Ultimate analysis [weight%, dry ash free basis]	
Nitrogen	1.72
Carbon	40.70
Hydrogen	5.35
Sulfur	1.23
Oxygen	42.25
Higher heating value [MJkg^{-1}]	15.65
Lower heating value [MJkg^{-1}]	14.45

The inorganic elements in the demineralized poultry litter were measured using the handheld portable X-ray fluorescence machine (Olympus Delta-50 Premium, USA) under the Geochem method, and the results were recorded in Table 2.

Table 2 Inorganic elements composition in the demineralized poultry litter.

Element	Content [%]	Element	Content [%]
Silicon	1.13	Calcium	3.57
Phosphorus	0.50	Aluminum	1.89
Sulphur	0.48	Iron	0.75
Chlorine	0.72	Chromium	0.05
Potassium	2.27	Manganese	0.14
Copper	0.04	Zinc	0.08

2.2. Pyrolysis experimental set-up and procedure

The pyrolysis experiment was conducted in a laboratory-scale fixed bed reactor in the Department of Chemical Engineering at Botswana International University of

Science and Technology, Palapye, Botswana. The pyrolysis reactor consisted of the following components: fixed bed reactor (TK01), condensers (TK02, TK03, and TK04), and incondensable gaseous holder (TK05), as shown in Fig. 1. The condensers TK02 and TK03 were used to recover the aqueous oil phase, and TK04 recovered the organic condensate. The steel tube (ID: 0.06 m and H: 0.6 m) was inserted inside a vertical muffed tube electrical furnace, and upon the pyrolysis, the gases produced travelled through the condensers (coolant at 20 °C), and condensable gases were converted to liquid bio–oils while the incondensable gases were kept in the incondensable gaseous holder.

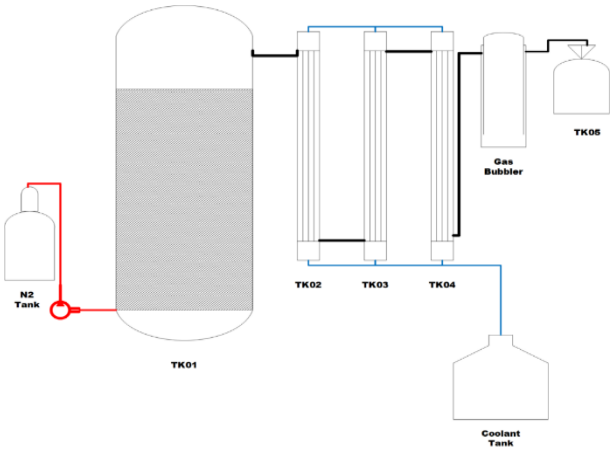

Fig. 1 Pyrolysis machine schematic layout.

Prior to the pyrolysis reaction, N_2 gas was flashed into the reactor for 15 min at 101.3kPa to create an inert environment. A known mass of the demineralized poultry litter was loaded into the reactor, and the operating parameters (temperature, particle size, and reaction time) were set with reference to the Response Surface Methodology Central Composite Design experimental matrix, as explained in Section 2.3. After each run, the reactor was switched off and cooled to room temperature before removing the biochar in the fixed bed reactor chamber (TK01). The biochar was weighed and calculated under a dry basis, as shown in Equation 1, to establish the biochar yield (BY) [15]

$$BY = \frac{W_F}{W_O} \times 100\% \qquad (1)$$

where W_F is the biochar weight, and W_O is the demineralized poultry litter weight.

2.3. Response surface methodology design matrix

Response Central composite design (CCD) optimizing tool of the response surface methodology was used to determine the optimum pyrolysis parameters that yield maximum biochar with high quality. This study used Stat-Ease Design Expert software version 13.0.5.0 to formulate the CCD matrix. A total of 20 experimental sets were formulated, including 6 axial points, 6 replicate points, and 8 factorial points. Three independent process parameters selected were temperature (A), particle size (B), and reaction time (C), with 5 different levels as shown in Table 3. Particle sizes were segmented into different sizes using a sieve according to ISO 585/3310-1 mesh sizes [25]. The data of the input parameters were normalized by converting the uncoded to coded values using Equation 2 [19].

$$X_{coded} = \frac{X_{real} - X_{average}}{\Delta X} \qquad (2)$$

where X_{coded} is the coded values of the independent variables, X_{real} is the real value of the independent variable in uncoded units, $X_{average}$ is the average of the low and high values for independent variables, ΔX = step change.

Biochar yield (BY), higher heating value (HHV), hydrogen-to-carbon ratio (H/C ratio), and energy yield (EY) were the selected responses, understudy. Biochar HHV was measured using a bomb calorimeter (Supercal2, South Africa) according to ASTM D5865–12 standard [24]. The H/C ratio was determined by first determining the biochar's elemental composition (CHNS/O) and derive the hydrogen-to-carbon ratio (H/C ratio). The elemental composition was measured using the elemental analyzer (Thermo scientific flash 2000 CHNS/O, USA) according to ASTM D5291–96 standard for CHNS contents [23]. Then the oxygen content was determined by subtracting CHNS constituents from 100 as shown in Equation 3. The EY was calculated using Equation 4 [19].

$$O = 100 - (C + H + N + S + Ash)\% \qquad (3)$$

$$EY = \frac{HHV_F}{HHV_O} \times BY(\%) \qquad (4)$$

where HHV_F is the higher heating value of biochar, and HHV_O is the higher heating value of demineralized poultry litter. The following regression model was used to estimate the mathematical correlations between three independent variables and each response as expressed in Equation 5.

Table 3 Experimental factors and coded levels for independent variables used in the CCD matrix.

Variable	Coded	-1.682	-1	0	+1	+1.682
Temperature [°C]	A	214.80	300.00	425.00	550.00	635.22
Particle size [mm]	B	0.03	1.17	2.84	4.51	5.66
Time [min]	C	4.77	15.00	30.00	45.00	55.22

Table 4 Central Composite Design experimental design matrix and the responses.

Run	Temperature [°C]	Particle size [mm]	Reaction time [min]	Biochar yield [%]	HHV [MJKg^{-1}]	H/C ratio	Energy Yield [%]
1	550.00	1.17	45.00	44.45	11.97	0.03	33.99
2	425.00	2.85	4.77	37.92	21.47	0.04	52.01
3	550.00	1.17	15.00	43.23	12.92	0.03	35.69
4	214.78	2.85	30.00	79.78	17.24	0.10	87.88
5	300.00	1.17	15.00	65.43	15.56	0.08	65.03
6	550.00	4.52	45.00	31.90	21.17	0.02	43.15
7	425.00	2.85	30.00	39.62	11.35	0.04	28.72
8	425.00	2.85	30.00	36.72	21.62	0.04	50.71
9	300.00	4.52	45.00	44.24	23.43	0.06	66.24
10	550.00	4.52	15.00	33.52	21.58	0.02	46.22
11	300.00	4.52	15.00	44.12	23.45	0.06	66.09
12	425.00	2.85	30.00	37.30	21.62	0.04	51.53
13	425.00	5.66	30.00	34.01	23.26	0.03	50.54
14	425.00	2.85	55.23	36.46	20.45	0.03	47.64
15	425.00	2.85	30.00	37.11	22.35	0.04	52.99
16	425.00	2.85	30.00	36.43	16.11	0.04	37.50
17	425.00	2.85	30.00	34.94	24.28	0.04	54.20
18	300.00	1.17	45.00	57.82	14.32	0.08	52.91
19	635.22	2.85	30.00	34.79	19.89	0.02	44.20
20	425.00	0.03	30.00	60.00	6.82	0.05	26.14

$$Y = \beta_0 + \sum_{i=1}^{k} \beta_i X_i + \sum_{i=1}^{k} \beta_{ii} X_i^{\,2} + \sum \sum_{i=1}^{k} \beta_i X_i X_j + \varepsilon \quad (5)$$

where Y is the predicted response (BY, HHV, H/C, and EY), X_i and X_j are the input parameters (A, B and C), and b is the regression coefficient, o, i, j are the intercept, linear and quadratic effects, k and $\mathcal{E}$ are the number of parameters and random error.

After inserting the experimental response variables into the CCD design matrix (Table 4), models were generated. The validity of the constructed models was evaluated using the analysis of variance method (ANOVA). The degree of model fitting was assessed using correlation coefficients (R^2), lack–of–fit test, and the significance level of 0.05 using probability values (*p-values*) and Fisher's test values (F-values). The contour plots (2D), response surface plots (3D), and residual plots were developed from the models. Derringer's desirability method provided in the Stat-Ease Design Expert software version 13.0.5.0 was used on each model to determine the optimum independent variable parameters that can provide optimum performance values of the intended responses.

3. Results and discussion

3.1. Models for biochar production

The response results of biochar yield, higher heating value, H/C ratio, and energy yield were inserted into the Stat-Ease Design Expert software version 13.0.5.0 as output response 1–4 respectively into the proposed design discussed in Section 2.3 and shown in Table 4. These results were used to develop empirical models expressed in terms of coded factors (Equations 6–9).

$$BY = 36.76 - 13.38A - 7.39B - 0.76C + 1.58AB + 6.76A^2 + 3.11B^2 + 6.06AB^2 \quad (6)$$

$$HHV = 18.54 - 0.3423A + 4.58 - 0.3165C \quad (7)$$

$$H/C = +0.0370 - 0.0251A - 0.0060B - 0.0011C + 0.0019AB + 0.0001AC + 0.0012BC + 0.0074A^2 + 0.0023B^2 - 0.0002C^2 \quad (8)$$

$$EY = +46.98 - 12.06A + 5.50B - 1.76C + 6.86A^2 - 2.93B^2 \quad (9)$$

The models with coded factors are used to predict the output response at any given level of each process parameter. In addition, the coefficient factors in each model signify the relative impact of each process parameter on the response. It can be observed from Equations 6–9 that the linear coefficients of temperature (A) have a negative effect on the BY, HHV, H/C ratio, and EY. Particle size (B) has a negative effect on the BY and H/C ratio but positive effect on HHV and EY. The reaction time (C) had a negative effect on the BY, HHV, H/C ratio, and EY. Quadratic coefficients of temperature (A^2) had a positive effect on the BY, H/C ratio, and EY. The quadratic particle size (B^2) had positive effect on the BY and H/C ratio and negative effect on the EY. The quadratic effect reaction time (C^2) had negative effect on the H/C ratio response. The interaction of temperature and particle (AB) size had positive effect on the BY and H/C ratio. That of AC and BC had positive effect on the H/C ratio.

BY was observed to be affected positively by the quadratic interaction of AB^2. The interaction of temperature, particle size, and reaction time has significant effect on biochar production through the pyrolysis process of the demineralized poultry litter. The process parameters were analyzed for their significance to the above developed models, and their variance were discussed in the subsequent sections.

3.2. Statistical analysis of the responses

To validate the experimental results and the models developed above, the analysis of variance using ANOVA was applied in testing for significance on all the models and validated statistically using the Fisher test value (F-value), *p–value*, and lack of fit as shown in Table 5. The developed regression models of BY, HHV, H/C ratio, and EY had higher F-values of 93.27, 8.77, 307.25, and 14.24, respectively, with a *p–value* < 0.0001 except for HHV, which has a *p–value* < 0.0011. This means that they are 0.01% chance (BY, H/C ratio, EY) and 0.11% chance (HHV) that the models F–value might occur due to noise hence making all the regression models significant [18]. The F–value compares the developed regression model's mean square value and the residuals' mean square values (i.e., error) [19]. Therefore, the F–value and sum of squares should be higher while the *p–value* should be lower. This ensures the developed model is reliable and can be reproduced while maintaining a good relationship between the response and the independent variables [15]. The F–values (along with *p–values*) of lack of fit for BY, HHV, H/C ratio, and EY are 2.65 (0.1504), 0.22 (0.9818), 2.25 (0.1972) and 0.12 (0.9970). The lack of fit developed from all the models are insignificant, all with a *p–value* > 0.05, and they are 15.04%, 98.18%, 19.72%, and 99.70%, respectively, that the F-value might occur due to noise. The lack of fit shows the inadequacy of the regression model in explaining the experimental data in the sphere at the points not included in the regression [26]. Therefore an insignificant lack of fit shows that the model fits the data well and is the desired fit [26].

Table 5 ANOVA for the fitted models.

Source	Sum of square	df	Mean Square	F–value	*p–value*
Biochar yield					
Model	2966.20	7	423.75	93.27	<0.0001
Residual	54.52	12	4.54		
Lack of Fit	42.94	7	6.13	2.65	0.1504
Pure error	11.57	5	2.31		
Cor Total	3020.75	19			
Higher Heating Value					
Model	289.11	3	96.37	8.77	0.0011
Residual	175.89	16	10.99		
Lack of Fit	58.06	11	5.23	0.22	0.9818
Pure error	117.83	5	23.57		
Cor Total	465.00	19			
H/C ratio					
Model	0.01	9	0.00	307.25	<0.0001
Residual	0.00	10	0.00		
Lack of Fit	0.00	5	0.00	2.25	0.1972
Pure error	0.00	5	0.00		
Cor Total	0.01	19			
Energy yield					
Model	3311.82	5	662.36	14.24	<0.0001
Residual	651.39	14	46.53		
Lack of Fit	111.86	9	12.43	0.12	0.9970
Pure error	539.53	5	107.91		
Cor Total	3963.21	19			

where: *p-value* < 0.05 is significant, df: Degree of freedom.

Table 6 Model summary statistics for biochar yield, higher heating value, H/C ratio and energy yield.

Source	Standard deviation	Mean	Coefficient of variation [%]	Included significant factors only			Adequate precision
				R^2	Adjusted R^2	Predicted R^2	
Biochar yield	2.13	43.49	4.90	0.98	0.97	0.85	33.82
Higher heating Value	3.32	18.54	17.88	0.62	0.55	0.50	10.38
H/C ratio	0.00	0.04	4.37	0.99	0.99	0.98	62.80
Energy yeild	6.82	49.67	13.73	0.84	0.78	0.75	15.32

Table 7 ANOVA results for the parameters in the models.

Source	Sum of square	df	Mean Square	F–value	*p–value*
Biochar yield					
A-Temperature	1012.06	1	1012.06	222.76	< 0.0001
B-Particle size	744.92	1	744.92	163.96	< 0.0001
C-Reaction time	7.81	1	7.81	1.72	0.2144
AB	19.99	1	19.99	4.40	0.0578
A^2	661.95	1	661.95	145.70	< 0.0001
B^2	140.66	1	140.66	30.96	0.0001
AB^2	121.81	1	121.81	26.81	0.0002
Higher heating value					
A-Temperature	1.60	1	1.60	0.15	0.7078
B-Particle size	286.14	1	286.14	26.03	0.0001
C-Reaction time	1.37	1	1.37	0.12	0.7289
H/C ratio					
A-Temperature	0.01	1	0.01	2380.17	< 0.0001
B-Particle size	0.00	1	0.00	136.42	< 0.0001
C-Reaction time	0.00	1	0.00	4.40	0.0623
AB	0.00	1	0.00	7.92	0.0183
AC	0.00	1	0.00	0.04	0.8406
BC	0.00	1	0.00	3.22	0.1032
A^2	0.00	1	0.0008	218.57	< 0.0001
B^2	0.00	1	0.0001	21.47	0.0009
C^2	0.00	1	0.00	0.10	0.7633
Energy yield					
A-Temperature	1985.89	1	1985.89	42.68	< 0.0001
B-Particle size	413.04	1	413.04	8.88	0.0099
C-Reaction time	42.47	1	42.47	0.90	0.3556
A^2	685.42	1	685.42	14.73	0.0018
B^2	125.01	1	125.01	2.69	0.1235

where: *p-value* < 0.05 is significant, df: Degree of freedom.

Table 6 further verified the adequacy of the developed models by determining the standard deviation, mean, R^2 values and adequate precision. A low standard deviation reflects that the model is well suited for optimization hence making the model more desirable and good [27]. All the developed models for BY, HHV, H/C ratio, and EY had a low standard deviation at 2.13, 3.32, 0.00, and 6.82, respectively, indicating that the models are well suitable for optimization. The mean values for BY, HHV, H/C ratio, and EY were at 43.49, 18.54, 0.04, and 49.67, respectively, with small coefficient of variation at 4.90%, 17.88%, 4.37%, and 13.73% respectively, showing a small percentage error on the mean values. This indicates that the values that constitute mean values deviate from each other at a small fraction making the models good for reproducibility [26]. The coefficient of determination indicates a model's adequacy, accuracy, and availability, giving it significance and quality for application. The model's coefficient of determination (R^2) should be close to 1, indicating a perfect fit of the model to the data [28]. Further, the corrected goodness–of–fit (Adjusted R^2) recognizes the percentage of difference in the design points explained by the model's input data. The models for BY, HHV, H/C ratio and EY had strong correlation coefficients at 0.98, 0.62, 0.99 and 0.84 and the difference between the R^2 and Adjusted R^2 were 0.01, 0.07, 0.00 and 0.06 implying that a small fraction of the total variation cannot be explained by the models respectively.

Also, the difference between the Adjusted R^2 and the Predicted R^2 on all models was less than 0.2 (0.12, 0.05, 0.01 and 0.03) meaning that the Adjusted R^2 is in reasonable agreement with the Predicted R^2. The Adequate precision values for all the models were greater than 4 which indicates an adequate signal that is desirable hence all the models are effective to be used to navigate the design space.

Table 7 shows the ANOVA results of the model terms. The term with a *p–value* of less than 0.0500 is significant and values greater than 0.050 are not significant to the regression model. As shown in Table 7, the linear, square, interaction terms and square interaction terms were significant in every model except for the following terms in each model (non–significant terms): BY (C), H/C ratio (AC, BC and C^2) and EY (C and B^2).

The graphical presentation of the predicted and the actual values of models for BY, HHV, H/C ratio, and EY are shown in Fig. 2a–d. The prediction and actual responses on all the models (BY, HHV, H/C ratio, and EY) have an almost linear relationship with a negligible variation. This shows a strong correlation between the model for the prediction and actual values making the model reliable and applicable in predicting the responses under study. A desired model should have a close relationship with the experimental data [37]. The effect of each independent variable on the response is determined by plotting these variables on the perturbation graphs.

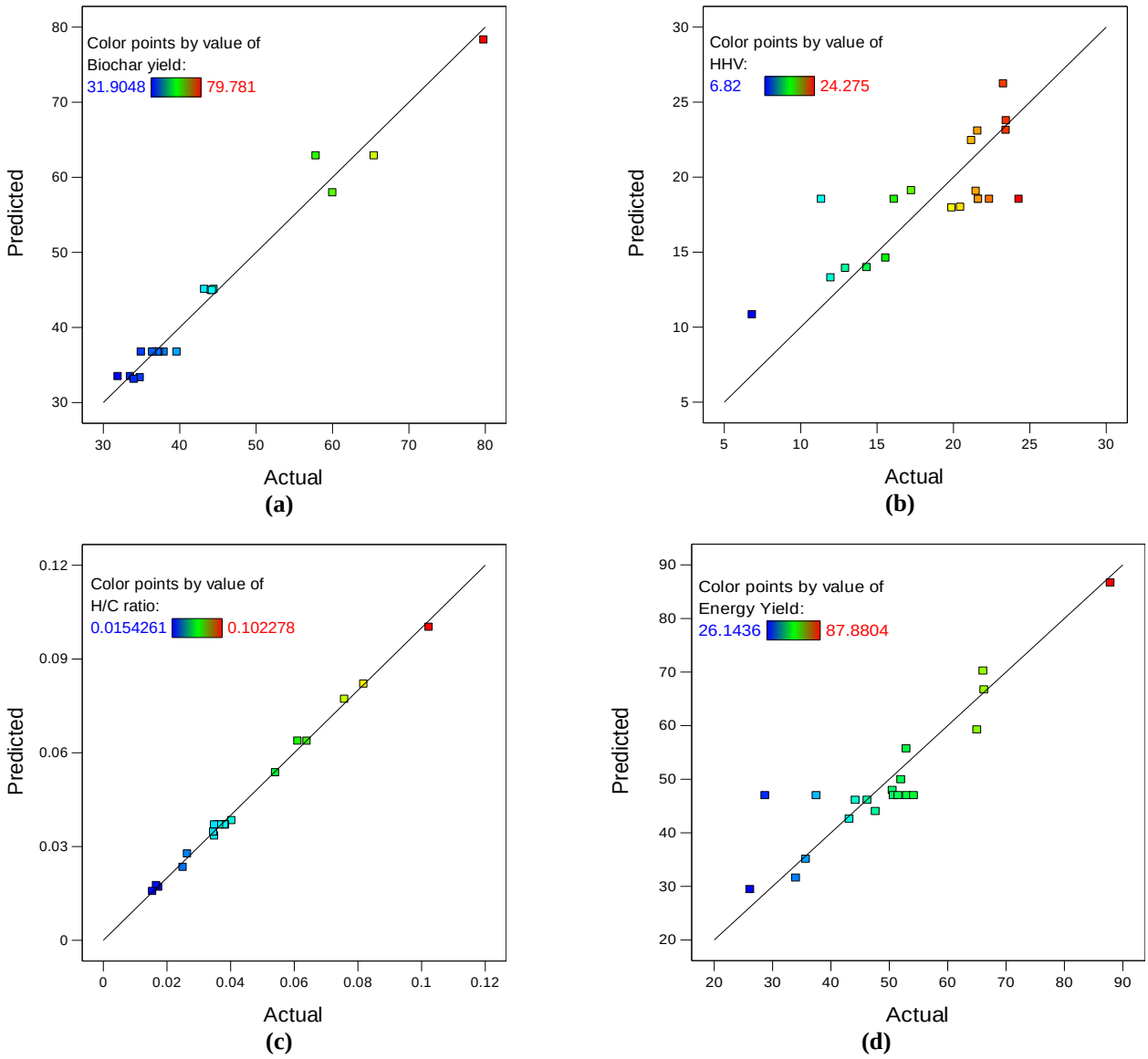

Fig. 2 Actual vs predicted values of the model: (a) biochar yield, (b) higher heating value, (c) H/C ratio, and (d) energy yield.

The perturbation plots identify which independent variable is most effective to the response by shifting only one factor (the one whose effect is required), while others are constant. The perturbation plot is done by identifying the reference point and adjusting the range at the center of each independent variable. Next, a plot of the response versus the deviation of the independent variables from the reference point is done to study their sensitivity to the response. A flat line on the plot indicates that the independent parameter has the least effect on the response, while a curvature or step slop has the most effect on the response [18]. As shown in Fig. 3a, the order of the independent variables to biochar yield response from the most to the least effective is as follows: temperature (A), particle size (B), and reaction time (C). This implies that temperature (A) gives the most response compared to particle size (B) and reaction time (C) in producing a high yield of biochar. In Fig. 3b, on the higher heating value, particle size (B) had the most effective response compared to the temperature (A) and reaction time (B), which had an almost flat line indicating the least effective parameters to this response. On the H/C ratio output (Fig. 3c), temperature (A) followed by particle size (B) had the most significant effect on the response. Reaction time (C) had an almost flat line indicating that its effect on the H/C ratio response is negligible. In Fig. 3d, temperature (A) and particle size (B) had the most effective response to the energy yield response compared to the reaction time (C), which had an almost flat line.

The normality assumption is established by plotting normal probability vs residuals graphs validating the models. Residuals demonstrate how well the ANOVA assumption is met, whereas internally studentized residuals estimate the standard deviation as a function of the actual and predicted values [29].

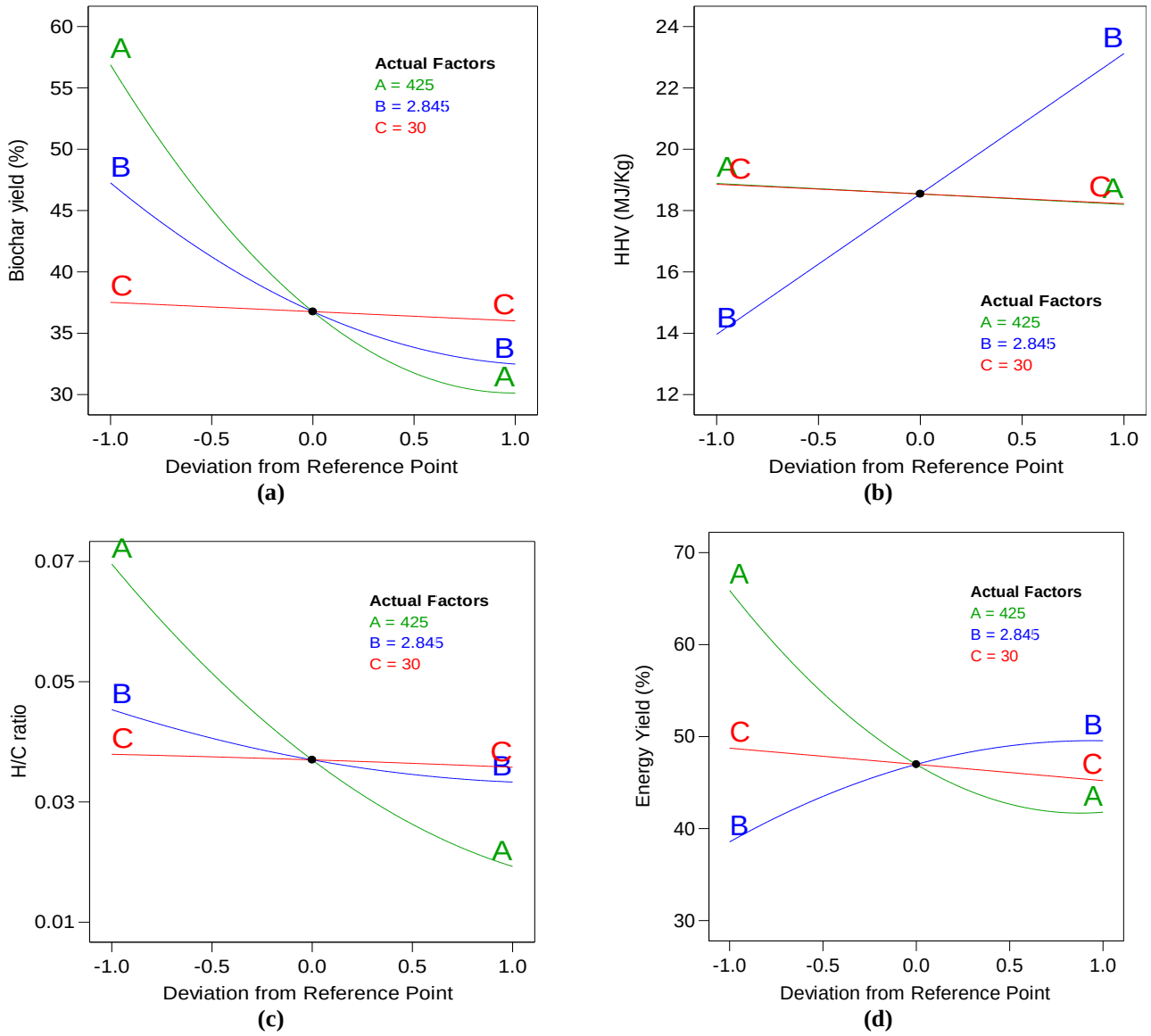

Fig. 3 Perturbation plots for: (a) biochar yield, (b) higher heating value, (c) H/C ratio, and (d) energy yield

A straight line on the normal probability of experimental residuals is desired for the normality of the assumption to be satisfied [30]. Fig. 4a–d in the supplementary data shows the normal probability plots of biochar yield, higher heating value, H/C ratio, and energy yield respectively. These plots demonstrate that the points on the plots follow a straight line, indicating that the residuals are normally distributed, and the normality assumption is therefore supported.

3.3. Contour plots parametric interaction of process variables in the model

The interaction effect of independent variables on the process parameter output is explained best by studying the pattern behavior of contour plots [19]. In addition, contour plots help in obtaining optimum process parameters. Subsections 3.3.1–3.3.4 explain the parametric interaction of the independent variables within the models using the contour plots. The optimum region to a particular desired response is noted with a red dot inside the small ellipses contour plot.

Parametric interaction of the independent variables on the biochar yield model

The interaction of pyrolysis temperature (A) and poultry litter particle size (B) has a significant effect on the biochar yield produced, as noted by the contour plots in Fig. 5a–b. At a fixed reaction time of 30 min, an increase in temperature from 300 to 550.00 °C and particle size from 1.17 to 4.52mm decreases the biochar yield from 60 to 30%. This reduction of biochar yield may be due to the thermal decomposition of the lignocellulosic compound such as lignin, cellulose, and hemicellulose, combustion, increased volatiles in the organic matter, and the dehydration of hydroxyl compounds [15].

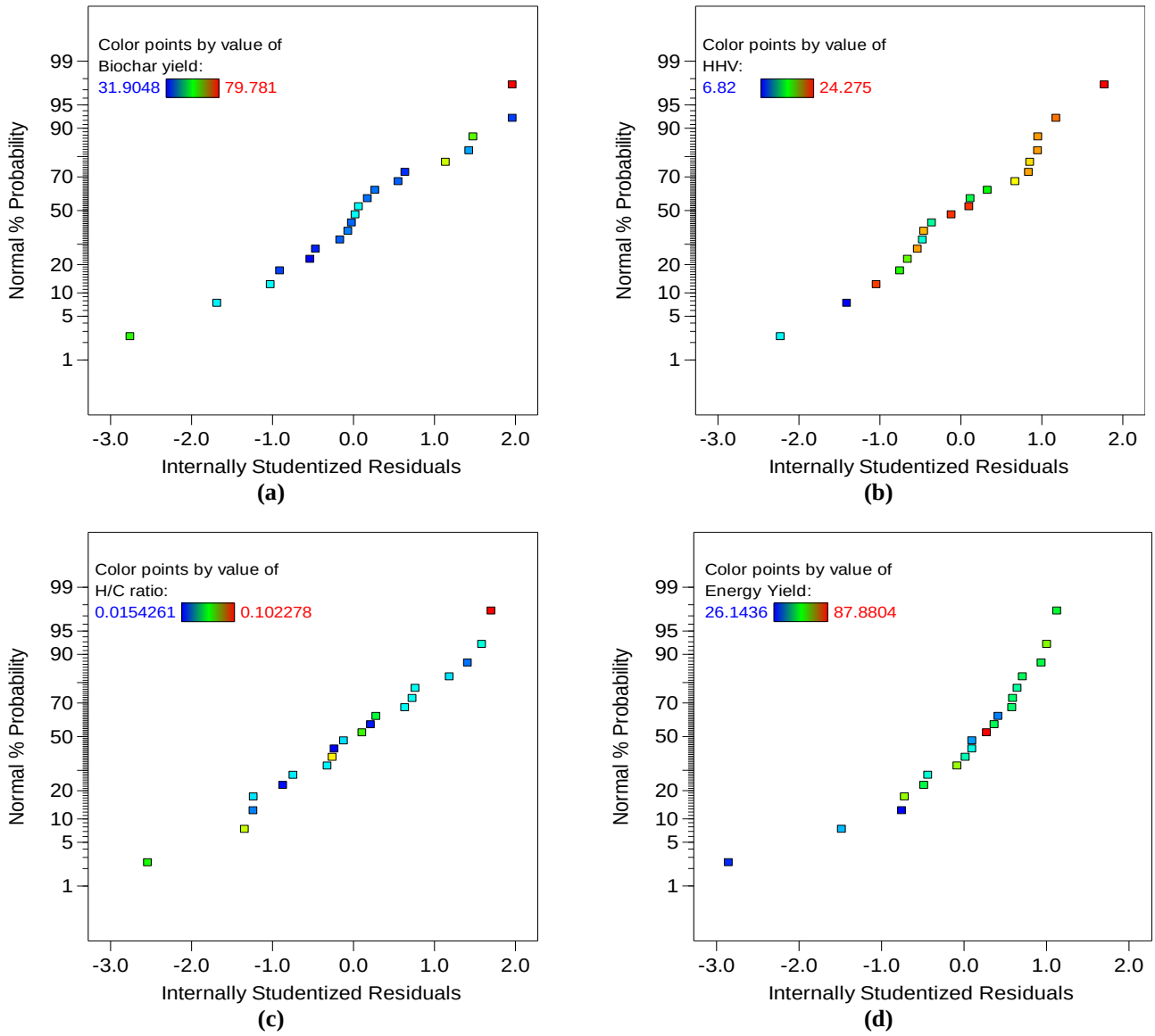

Fig. 4 The studentized residual and normal percentage for: (a) biochar yield, (b) higher heating value, (c) H/C ratio, and (d) energy yield

Lee et al. [15] investigated the pyrolysis of palm kernel shells and empty fruit bunch and noted a decrease in biochar yield as the temperature increased [15]. Arafat Hossain et al. [18] also showed that higher temperatures reduced biochar output during pyrolysis.

Biomass particle size affects the rate at which heat is transferred into the biomass during pyrolysis. Hence a need to study its simultaneous interaction if of importance. Sensoz et al.[31] investigated the effect of particle size on rapeseeds at 500.00 °C on biochar yield. An increase in particle size from 0.22 to 0.85mm decreased the biochar yield from 22.18 to 20.44%. However, at particle sizes above 1.8mm, the biochar decreased. A similar effect was also reported by Şensöz and Kaynar [32], who observed a decrease in biochar yield with the increase in particle size at 400.00 °C temperature. Other researchers [33,34] noted a decrease in biochar yield when particle size increased. Time did not affect the biochar yield. This finding was in agreement with other researchers who found out that reaction time does not affect the biochar yield [35–37].

Reaction time had no significant effect on the biochar yield. High biochar yield is favored when reaction time is prolonged from hours to days at low temperatures giving time for the biomass to undergo secondary and polymerization reactions that favors more yield [20]. The reaction time (4.77–55.22 min) in the study was insufficient to have a significant effect on the biochar yield. However, Mukherjee [38] noted a decrease in biochar yield when the reaction time increased from 20.00 to 90.00 min under varying temperature conditions. The role of reaction time is often dominated by temperature, and this makes the analysis of the effect of reaction time on biochar yield difficult to comprehend.

Parametric interaction of the independent variables on higher heating value model

The effect of pyrolysis temperature (A) and poultry litter particle size (B) on the biochar's higher heating value is shown in Fig. 6a–b. It can be observed from these graphs that temperature had little effect on the higher heating value, while an increase in particle size had a continuous increase in the higher heating value. This observation is justified by how we prepare the poultry litter samples for pyrolysis. Poultry litter comprises cellulose, hemicellulose, and lignin material which contain high oxygen content, high volatile matter, and fixed carbon composition. When fractioned into different particle size samples, the materials' proportion will not be distributed uniformly. For example, a small-sized fractioned sample is composed mainly of manure that contains cellulose and hemicellulose materials which have high oxygen and volatiles; hence on combustion, they will produce a lower higher heating value as compared to a fractioned sample with a large particle size composed mainly of woody bedding material constituting mostly the lignin material that has the fixed carbon. Our findings were in agreement with El Hanandeh et al. [39], who noted that different compositions of biomass material (cellulose, hemicellulose, and lignin) affected the higher heating value. For example, deseeded carob pod biomass has 79.00% of carbohydrates had a higher heating value compared to oak acorn shell (56.00% hemicellulose) and oak acorn shell (54.00% cumulative hemicellulose and cellulose) [39].

Reaction time had no significant effect to the higher heating value. Suman and Gautam [40] was in agreement with our findings noting a non–significant effect of reaction time on higher heating value (rice husk and wooden dust feedstocks). Chiou [41] noted a decrease in higher heating value when reaction time increased (apple feedstock) while Mundike [42] noted an increase in higher heating value when reaction time increased (*Lantan camara* feedstock). Therefore, the effect of reaction time on higher heating value is difficult to interpret hence each study analysis its effect.

Parametric interaction of the independent variables on H/C ratio model

The interaction of the independent variables with the H/C ratio response is shown in Fig. 7. A low H/C ratio in biochar is desired as it offers the fuel a higher degree of aromaticity, stability, and carbonization level [43]. This means the fuel will have a long shelf life without oxidizing with high C–C bonds compared to C–H and C-O bonds [15]. Fig. 7a-b shows the 2D and 3D interaction graphs of temperature (A) and particle size (B) to the H/C ratio in the biochar. An increase in temperature and particle size decreased the H/C ratio. These findings were in agreement with Manya et al. [44], who noted a decrease in the H/C ratio when the temperature and particle size increased [44]. Fig. 7c–d shows the particle size and temperature interaction level to the H/C ratio in 2D and 3D models, respectively. As particle size and time increased, the H/C ratio decreased. Reaction time should be long to ensure high efficiency in the carbonization process, especially when the inter and intra–particle heat transfer is insignificant. Abbas et al. [33] reported that for biochar to produce a low H/C ratio with high carbonization efficiency, aromatic degree, and good stability, the reaction time should be over 90 min [33]. Rection time had an insignificant effect to the H/C ratio of the biochar. Reaction time does not promote the dehydration and deoxygenation process [45]

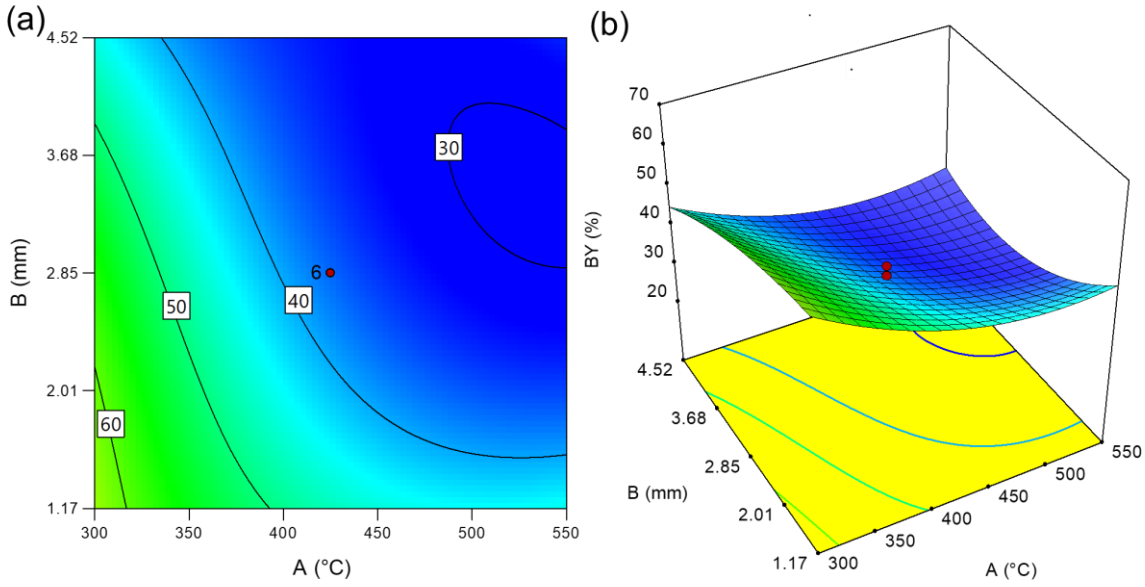

Fig. 5 Model graphs of biochar yield at a fixed reaction time (C) of 30.00 min: (a) 2D contour plot (b) 3D response surface.

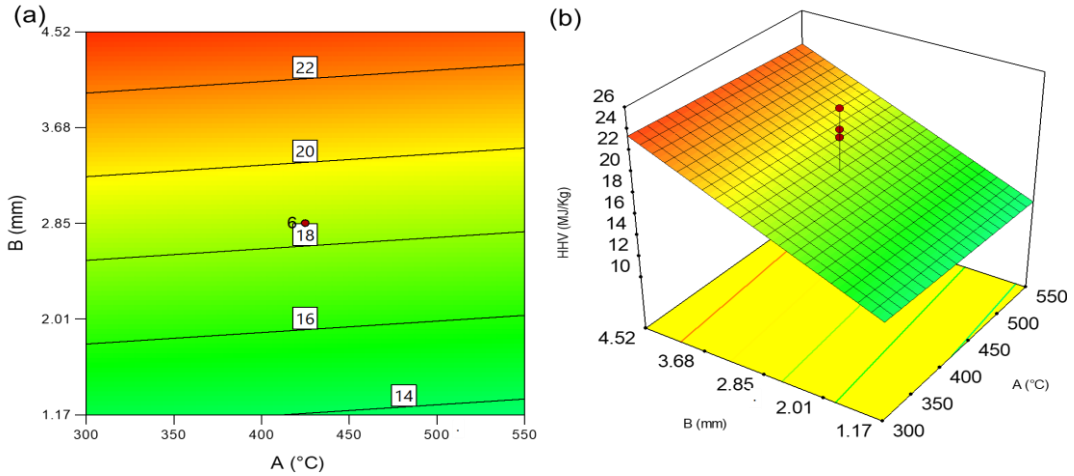

Fig. 6 Model graphs of higher heating value at a fixed reaction time (C) of 30 min: (a) 2D contour plot (b) 3D response surface

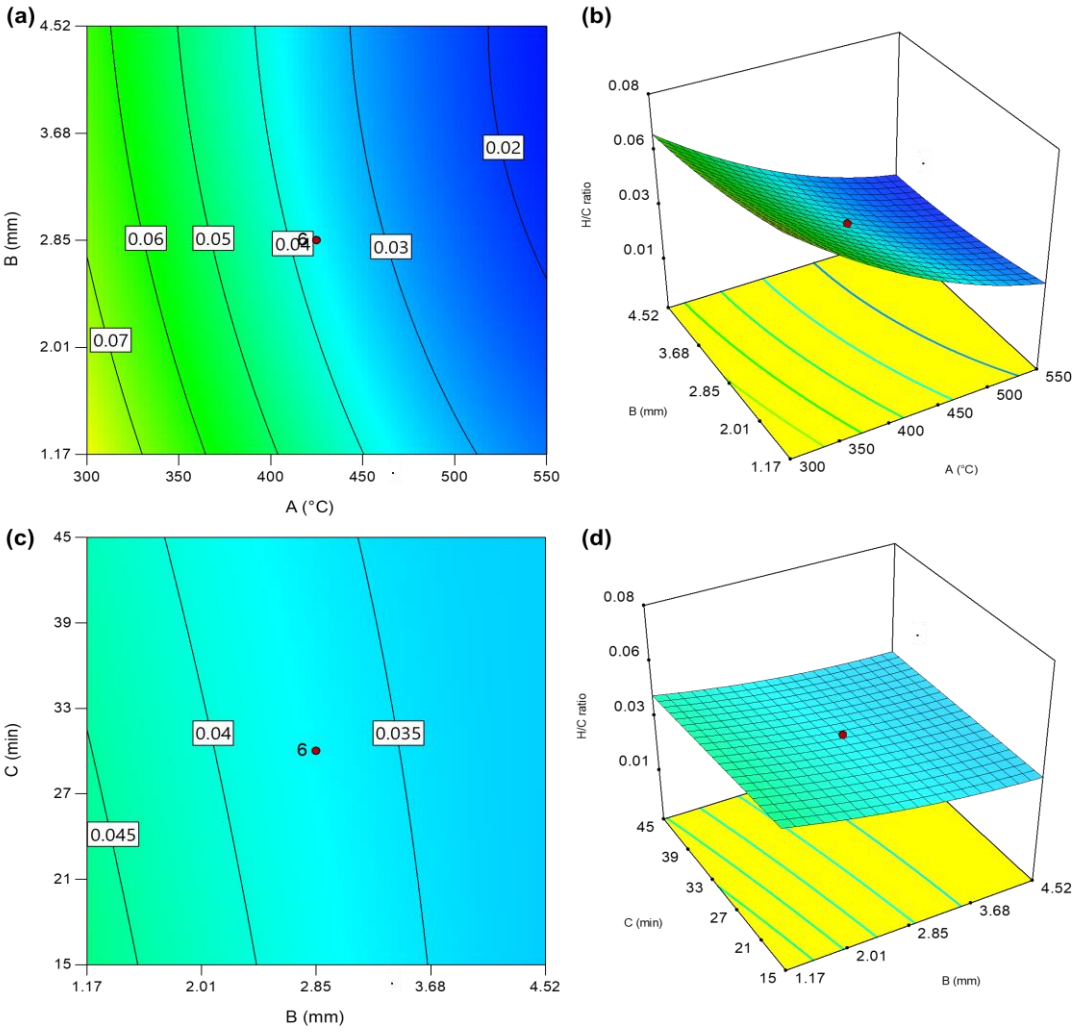

Fig. 7 Model graphs contour plot of H/C ratio in: (a) 2D for A and B at fixed C of 30.00 min (b) 3D for A and B at fixed C of 30 min (c) 2D for B and C at fixed A of 425.00 °C (d) 3D for B and C at fixed A of 425.00 °C.

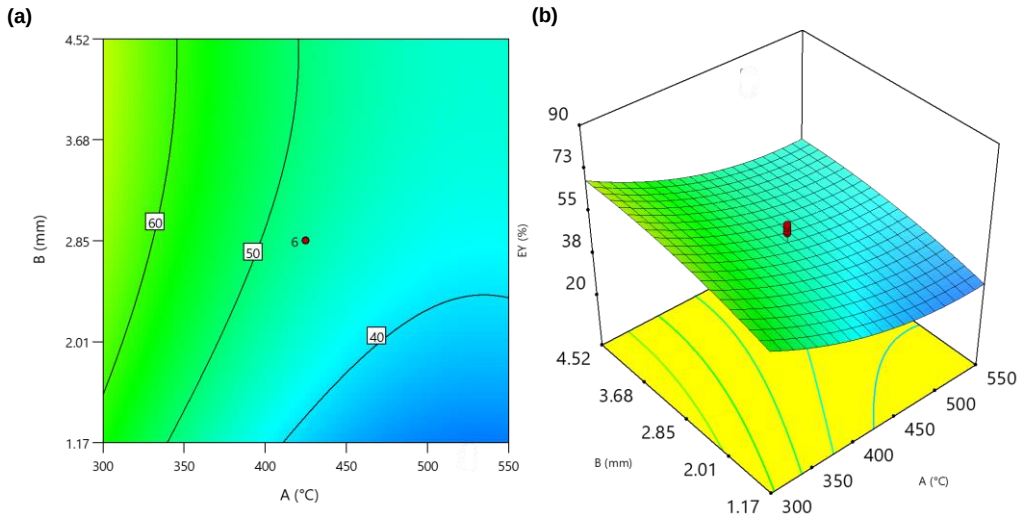

Fig. 8 Model graphs of energy yield at a fixed reaction time (C) of 30.00 min: (a) 2D contour plot (b) 3D response surface

Table 8 Predicted vs experimental yield of BY, HHV, H/C ratio and EY on optimized pyrolysis parameters.

Main output	Validation	Process parameters			Desirability	BY [%]	HHV [MJkg^{-1}]	H/C ratio	EY [%]
		A [°C]	B [mm]	C [min]					
BY	Predicted	300.00	2.47	15.00	0.54	59.49	18.18	0.07	66.00
	Experiment					61.06	17.80	0.07	69.00
	Deviation [%]					2.57	2.13	0.00	4.97
HHV	Predicted	300.00	4.05	15.00	0.53	49.69	22.48	0.07	70.00
	Experiment					50.34	21.60	0.07	69.00
	Deviation [%]					1.29	-4.07	0.00	-0.75
H/C ratio	Predicted	550.00	1.17	15.00	0.41	45.86	13.93	0.03	35.00
	Experiment					46.72	13.21	0.03	39.00
	Deviation [%]					1.84	-5.45	0.00	11.25
EY	Predicted	300.00	4.05	15.00	0.57	49.69	22.48	0.07	70.00
	Experiment					50.35	22.31	0.07	72.00
	Deviation [%]					1.31	-0.76	0.00	2.48

3.3.4 Parametric interaction of the independent variables in the energy yield model

It can be observed from Fig. 8a–b that a decrease in temperature and an increase in particle size increases the energy yield. A similar trend was observed by other researchers [19,46,47], who noted a continuous decrease in energy yield when temperature increased and particle size decreased. An increase in temperature cause the degradation of cellulose and hemicellulose through volatilization resulting in energy densification increase and biochar yield decrease making the energy yield to decrease [47]. Biomass particles with small sizes have high surface area and during pyrolysis the volatiles leave the reaction chamber fast without having time to thermal react resulting in low biochar yield hence causing the energy yield to decrease [33]. Energy yield is obtained by calculating biochar yield with higher heating value; therefore, their trend is in accordance with these mentioned responses [19]. Energy yield is dependent on the biochar yield and Higher Heating Value of the biochar, as noted above these parameters are non–significant making to the reaction time making energy yield also non–significant.

3.4. Optimization and validation of process parameters for the response outputs

An input and output relationship is important to develop models that can predict optimum response outputs. It is important to optimize the pyrolysis process of poultry litter to produce maximum biochar yield at an excellent quality. Regression models created using RSM can be applied to improve the process for production in this regard. The optimization process was performed to maximize the output of biochar yield, higher heating value, and energy yield and to lower the H/C ratio in the biochar. The higher heating value, energy yield, and H/C ratio maintains the quality while the biochar yield maximizes the production quantity. The Stat-Ease Design-Expert software suggested the optimum conditions while utilizing the desirability function option.

Table 8 summarizes the optimized process parameters of the response outputs in the study suggested by the

software. Experiments were done to validate the process parameters suggested by the software. To yield a maximum biochar yield of 59.49%, the temperature, particle size, and reaction time should be at 300 °C, 2.47mm, and 15 min, respectively, with desirability value of 0.54. Maximum higher heating value of 22.48MJKg^{-1}was achieved at optimized temperature, particle size, and time of 300 °C, 4.04mm, and 15 min, respectively, with desirability value of 0.53. A minimum H/C ratio of 0.03 was attained when temperature, particle size, and time were optimized to 550 °C, 1.17mm, and 15 min, respectively, with a desirability value of 0.41. A maximum energy yield of 70.00% was achieved when the temperature, particle size, and time were optimized at 300 °C, 4.04mm, and 15 min, respectively, with a desirability value of 0.57. According to the Harrington desirability function scale, a desirability value ranging from 0.4 to 0.6 is satisfactory, and one below 0.2 is unacceptable [48]. The ones in our regression models were above 0.4, which means they are satisfactory. To verify the models, experiments were carried out in accordance with their optimized pyrolysis parameters that yield the main output responses in study. Table 8 shows the deviation between the predicted and experimental to be less than 5.00% for the main output response in study with BY, HHV, H/C, and EY yielding 61.06%, 21.60MJkg^{-1}, 0.03, and 72.00% respectively under experimental procedure. Hence the experimental results confirm the models' suitability to be applied to predict output responses understudy.

4. Conclusions

In this study, the main objective was to develop models that can optimize the pyrolysis parameters to yield maximum biochar yield, maximum higher heating value, lower H/C ratio and maximum energy yield. RSM–CCD method was efficient in developing the empirical models and optimizing the pyrolysis parameters for biochar production. ANOVA showed models high F–values of biochar yield (93.27%), higher heating value (8.77 MJkg^{-1}), H/C ratio (307.25) and energy yield (14.24%) with a significant *p–value<0.0011*. This means there is 0.01% chance that the models F–value might be due to noise thereby making the models significant. In addition, the models lack–of–fit were insignificant *p–value > 0.05* hence it fits the experimental data to a desired fit. The models for biochar yield, higher heating value, H/C ratio and energy yield had a low standard deviation of 2.13, 3.32, 0.00, and 6.82 respectively making the models desirable for optimization with a low mean error of less than 18.00% making the models to be reproduced. The models for biochar yield, higher heating value, H/C ratio and energy yield had strong correlation coefficients at 0.98, 0.62, 0.99 and 0.84 and the difference between the R^2 and Adjusted R^2 were 0.01, 0.07, 0.00 and 0.06 implying that a small fraction of the total variation cannot be explained by the models respectively. The Adequate precision values for all the models were greater than 4 which indicates an adequate signal that is desirable hence all the models are effective to be used to navigate the design space. The contour and response surface plots identified interactions of the temperature, particle size and reaction time to the response outputs that had significant effect. Maximum biochar yield 59.49% was obtained at optimum parameters of 300 °C, 2.47mm, and 15.00 min. Maximum higher heating value 22.58MJkg^{-1} and energy yield 70.00% were obtained at optimum parameters of 300 °C, 4.04mm, and15.00 min. The H/C ratio 0.03 is lowest at optimum parameters of 550.00 °C, 1.17mm, and 15.00 min. The models and the experiments deviated by less than 5.00%. The results indicate a potential application of the models in predicting the response outputs in study when pyrolysis parameters are optimized.

Acknowledgments

The Authors appreciate the financial support of Botswana International University of Science and Technology under the S00392 research grant.

References

1. Enerdata, Total energy consumption, World Energy Clim. Stat. (2022). https://yearbook.enerdata.net/total-energy/world-consumption-statistics.html.
2. United Nations, World population prospects 2019, (2019). https://population.un.org/wpp/Publications/Files/WPP2019_DataBooklet.pdf.
3. F. Perera, K. Nadeau, Climate Change, Fossil-Fuel Pollution, and Children's Health, N. Engl. J. Med. 386 (2022) 2303–2314. https://doi.org/10.1056/nejmra2117706.
4. M.O. Oliveira, R. Somariva, O.H.A. Junior, J.M. Neto, A.S. Bretas, Biomass electricity generation using industry poultry waste, Int. Conf. Renew. Energies Power Qual. 1 (2012) 1650–1654. https://icrepq.com/icrepq'12/791-oliveira.pdf.
5. A. Lang, D. Bradley, G. Gauthier, Global bioenergy statistics 2021, (2021). https://www.worldbioenergy.org/uploads/211214 WBA GBS 2021.pdf.
6. OECD-FAO Agricultural outlook 2020-2029, OECD-FAO Agricultural Outlook 2020-2029, OECD, Rome, 2020.
7. Z. Yıldız, N. Kaya, Y. Topcu, H. Uzun, Pyrolysis and optimization of chicken manure wastes in fluidized bed reactor: CO2 capture in activated bio-chars, Process Saf. Environ. Prot. 130 (2019) 297–305. https://doi.org/10.1016/j.psep.2019.08.011.
8. A. Mohr, S. Raman, Lessons from first generation biofuels and implications for the sustainability appraisal of second generation biofuels, Effic. Sustain. Biofuel Prod. Environ. Land-Use Res. 63 (2015) 281–310. https://doi.org/10.1016/j.enpol.2013.08.033.
9. T. Komiyama, A. Kobayashi, M. Yahagi, The chemical characteristics of ashes from cattle, swine and poultry manure, J. Mater. Cycles Waste Manag. 15 (2013) 106–110. https://doi.org/10.1007/s10163-012-0089-2.

10. F.S. Dalólio, J. Nogueira, A. Cássia, C. De Oliveira, I. De, F. Ferreira, R. Christiam, M. De Oliveira, F. Teixeira, S. Teixeira, Poultry litter as biomass energy : A review and future perspectives, Renew. Sustain. Energy Rev. 76 (2017) 941–949. https://doi.org/10.1016/j.rser.2017.03.104.
11. S. V Vassilev, C. Braekman-Danheux, Characterization of refuse-derived char from municipal solid waste 1. phase-mineral and chemical composition, Fuel Process. Technol. 59 (1999) 135–161. https://doi.org/10.1016/s0378-3820(99)00018-1.
12. R. Fahmi, A. V. Bridgwater, I. Donnison, N. Yates, J.M. Jones, The effect of lignin and inorganic species in biomass on pyrolysis oil yields, quality and stability, Fuel. 87 (2008) 1230–1240. https://doi.org/10.1016/j.fuel.2007.07.026.
13. X. Liu, X.T. Bi, Removal of inorganic constituents from pine barks and switchgrass, Fuel Process. Technol. 92 (2011) 1273–1279. https://doi.org/10.1016/j.fuproc.2011.01.016.
14. Simbolon L.M (RCUK Centre for Sustainable Energy use in Food chains (CSEF)), Investigation of poultry litter conversion into useful energy resources using fast pyrolysis, (2019) 27–30. https://arro.anglia.ac.uk/id/eprint/704741.
15. X.J. Lee, L.Y. Lee, B.Y.Z. Hiew, S. Gan, S. Thangalazhy-Gopakumar, H.K. Ng, Valorisation of oil palm wastes into high yield and energy content biochars via slow pyrolysis: Multivariate process optimisation and combustion kinetic studies, Mater. Sci. Energy Technol. 3 (2020) 601–610. https://doi.org/10.1016/j.mset.2020.06.006.
16. W. Song, M. Guo, Quality variations of poultry litter biochar generated at different pyrolysis temperatures, J. Anal. Appl. Pyrolysis. 94 (2012) 138–145. https://doi.org/10.1016/j.jaap.2011.11.018.
17. K.T. Klasson, Biochar characterization and a method for estimating biochar quality from proximate analysis results, Biomass and Bioenergy. 96 (2017) 50–58. https://doi.org/10.1016/j.biombioe.2016.10.011.
18. M. Arafat Hossain, P. Ganesan, J. Jewaratnam, K. Chinna, Optimization of process parameters for microwave pyrolysis of oil palm fiber (OPF) for hydrogen and biochar production, Energy Convers. Manag. 133 (2017) 349–362. https://doi.org/10.1016/j.enconman.2016.10.046.
19. K. Anupam, A.K. Sharma, P.S. Lal, S. Dutta, S. Maity, Preparation, characterization and optimization for upgrading Leucaena leucocephala bark to biochar fuel with high energy yielding, Energy. 106 (2016) 743–756. https://doi.org/10.1016/j.energy.2016.03.100.
20. M.T.H. Siddiqui, S. Nizamuddin, N.M. Mubarak, K. Shirin, M. Aijaz, M. Hussain, H.A. Baloch, Characterization and Process Optimization of Biochar Produced Using Novel Biomass, Waste Pomegranate Peel: A Response Surface Methodology Approach, Waste and Biomass Valorization. 10 (2019) 521–532. https://doi.org/10.1007/s12649-017-0091-y.
21. I.Y. Eom, K.H. Kim, J.Y. Kim, S.M. Lee, H.M. Yeo, I.G. Choi, J.W. Choi, Characterization of primary thermal degradation features of lignocellulosic biomass after removal of inorganic metals by diverse solvents, Bioresour. Technol. 102 (2011) 3437–3444. https://doi.org/10.1016/j.biortech.2010.10.056.
22. I.M. Rajendra, I.N.S. Winaya, A. Ghurri, I.K.G. Wirawan, Thermogravimetric investigation of Reutealis Trisperma (Blanco) airy shaw and iron sand as bed material at different heating rates pyrolysis, J. Phys. Conf. Ser. 1450 (2020). https://doi.org/10.1088/1742-6596/1450/1/012098.
23. A.T. Tag, G. Duman, S. Ucar, J. Yanik, Effects of feedstock type and pyrolysis temperature on potential applications of biochar, J. Anal. Appl. Pyrolysis. 120 (2016) 200–206. https://doi.org/10.1016/j.jaap.2016.05.006.
24. I. Gravalos, D. Kateris, P. Xyradakis, T. Gialamas, S. Loutridis, A. Augousti, A. Georgiades, Z. Tsiropoulos, A study on calorific energy values of biomass residue pellets for heating purposes, For. Eng. Meet. Needs Soc. Environ. (2010) 1–9. https://www.formec.org/images/proceedings/2010/ab066.pdf.
25. Endecotts, Endecotts, (n.d.). www.endecotts.com.
26. L. Vera Candioti, M.M. De Zan, M.S. Cámara, H.C. Goicoechea, Experimental design and multiple response optimization. Using the desirability function in analytical methods development, Talanta. 124 (2014) 123–138. https://doi.org/10.1016/j.talanta.2014.01.034.
27. M.A. Bezerra, R.E. Santelli, E.P. Oliveira, L.S. Villar, L.A. Escaleira, Response surface methodology (RSM) as a tool for optimization in analytical chemistry, Talanta. 76 (2008) 965–977. https://doi.org/10.1016/j.talanta.2008.05.019.
28. S. Menard, Coefficients of determination for multiple logistic regression analysis, Am. Stat. 54 (2000) 17–24. https://doi.org/10.1080/00031305.2000.10474502.
29. M. Tripathi, A. Bhatnagar, N.M. Mubarak, J.N. Sahu, P. Ganesan, RSM optimization of microwave pyrolysis parameters to produce OPS char with high yield and large BET surface area, Fuel. 277 (2020) 118184. https://doi.org/10.1016/j.fuel.2020.118184.
30. S.I. Suárez-Vázquez, A. Cruz-López, J.M. Márquez-Reyes, H. Flores Breceda, C. García-Gómez, Comparative study of biochar prepared from cow dung and sewage sludge and its application as an adsorbent for organic pollutants removal in water, Environ. Prog. Sustain. Energy. 40 (2021). https://doi.org/10.1002/ep.13593.
31. S. Şensöz, D. Angin, S. Yorgun, Influence of particle size on the pyrolysis of rapeseed (Brassica napus L.): Fuel properties of bio-oil, Biomass and Bioenergy. 19 (2000) 271–279. https://doi.org/10.1016/S0961-9534(00)00041-6.

32. S. Şensöz, I. Kaynar, Bio-oil production from soybean (Glycine max L.); Fuel properties of Bio-oil, Ind. Crops Prod. 23 (2006) 99–105. https://doi.org/10.1016/j.indcrop.2005.04.005.
33. Q. Abbas, G. Liu, B. Yousaf, M.U. Ali, H. Ullah, M.A.M. Munir, R. Liu, Contrasting effects of operating conditions and biomass particle size on bulk characteristics and surface chemistry of rice husk derived-biochars, J. Anal. Appl. Pyrolysis. 134 (2018) 281–292. https://doi.org/10.1016/j.jaap.2018.06.018.
34. A. Demirbas, Effects of temperature and particle size on bio-char yield from pyrolysis of agricultural residues, J. Anal. Appl. Pyrolysis. 72 (2004) 243–248. https://doi.org/10.1016/j.jaap.2004.07.003.
35. H. Yeasmin, J.F. Mathews, S. Ouyang, Rapid devolatilisation of Yallourn brown coal at high pressures and temperatures, Fuel. 78 (1999) 11–24. https://doi.org/10.1016/S0016-2361(98)00119-7.
36. A.R. Mohamed, Z. Hamzah, M.Z.M. Daud, Z. Zakaria, The effects of holding time and the sweeping nitrogen gas flowrates on the pyrolysis of EFB using a fixed bed reactor, Procedia Eng. 53 (2013) 185–191. https://doi.org/10.1016/j.proeng.2013.02.024.
37. K.H. Kim, I.Y. Eom, S.M. Lee, D. Choi, H. Yeo, I.G. Choi, J.W. Choi, Investigation of physicochemical properties of biooils produced from yellow poplar wood (Liriodendron tulipifera) at various temperatures and residence times, J. Anal. Appl. Pyrolysis. 92 (2011) 2–9. https://doi.org/10.1016/j.jaap.2011.04.002.
38. A. Mukherjee, B.R. Patra, J. Podder, A.K. Dalai, Synthesis of Biochar From Lignocellulosic Biomass for Diverse Industrial Applications and Energy Harvesting: Effects of Pyrolysis Conditions on the Physicochemical Properties of Biochar, Front. Mater. 9 (2022) 1–23. https://doi.org/10.3389/fmats.2022.870184.
39. A. El Hanandeh, A. Albalasmeh, M. Gharaibeh, Effect of pyrolysis temperature and biomass particle size on the heating value of biocoal and optimization using response surface methodology, Biomass and Bioenergy. 151 (2021) 106163. https://doi.org/10.1016/j.biombioe.2021.106163.
40. S. Suman, S. Gautam, Effect of pyrolysis time and temperature on the characterization of biochars derived from biomass, Energy Sources, Part A Recover. Util. Environ. Eff. 39 (2017) 933–940. https://doi.org/10.1080/15567036.2016.1276650.
41. B. Sen Chiou, D. Valenzuela-Medina, C. Bilbao-Sainz, A.K. Klamczynski, R.J. Avena-Bustillos, R.R. Milczarek, W.X. Du, G.M. Glenn, W.J. Orts, Torrefaction of pomaces and nut shells, Bioresour. Technol. 177 (2015) 58–65. https://doi.org/10.1016/j.biortech.2014.11.071.
42. J. Mundike, F.X. Collard, J.F. Görgens, Torrefaction of invasive alien plants: Influence of heating rate and other conversion parameters on mass yield and higher heating value, Bioresour. Technol. 209 (2016) 90–99. https://doi.org/10.1016/j.biortech.2016.02.082.
43. K. Crombie, O. Mašek, S.P. Sohi, P. Brownsort, A. Cross, The effect of pyrolysis conditions on biochar stability as determined by three methods, GCB Bioenergy. 5 (2013) 122–131. https://doi.org/10.1111/gcbb.12030.
44. J.J. Manyà, M.A. Ortigosa, S. Laguarta, J.A. Manso, Experimental study on the effect of pyrolysis pressure, peak temperature, and particle size on the potential stability of vine shoots-derived biochar, Fuel. 133 (2014) 163–172. https://doi.org/10.1016/j.fuel.2014.05.019.
45. M.H. Mohd Hasan, R.T. Bachmann, S.K. Loh, S. Manroshan, S.K. Ong, Effect of Pyrolysis Temperature and Time on Properties of Palm Kernel Shell-Based Biochar, IOP Conf. Ser. Mater. Sci. Eng. 548 (2019). https://doi.org/10.1088/1757-899X/548/1/012020.
46. P. Basu, S. Rao, A. Dhungana, An investigation into the effect of biomass particle size on its torrefaction, Can. J. Chem. Eng. 91 (2013) 466–474. https://doi.org/10.1002/cjce.21710.
47. X.J. Lee, H.C. Ong, W. Gao, Y.S. Ok, W.H. Chen, B.H.H. Goh, C.T. Chong, Solid biofuel production from spent coffee ground wastes: Process optimisation, characterisation and kinetic studies, Fuel. 292 (2021) 120309. https://doi.org/10.1016/j.fuel.2021.120309.
48. H.W. Chen, W.K. Wong, H. Xu, An augmented approach to the desirability function, J. Appl. Stat. 39 (2012) 599–613. https://doi.org/10.1080/02664763.2011.605437.